An Asymmetric Dinuclear Bis(ansa-Zirconocene) Complex: Synthesis and Performance in Olefin (co-)Polymerization

Lars N. Jende, Thierry Roisnel, Virginie Cirriez, Alexandre Welle, Evgueni Kirillov, Jean-François Carpentier

catalysts

MDPI

Article

An Asymmetric Dinuclear Bis(*ansa*-Zirconocene) Complex: Synthesis and Performance in Olefin (co-)Polymerization

Lars N. Jende [1], Thierry Roisnel [2], Virginie Cirriez [3], Alexandre Welle [3], Evgueni Kirillov [1,*] and Jean-Francois Carpentier [1,*]

[1] Univ Rennes, CNRS, ISCR, UMR 6226, F-35700 Rennes, France
[2] Centre de Diffraction X, Univ Rennes, CNRS, ISCR, UMR 6226, F-35700 Rennes, France
[3] TotalEnergies, Zone Industrielle Feluy C, B-7181 Seneffe, Belgium; alexandre.welle@totalenergies.com (A.W.)
* Correspondence: evgueni.kirillov@univ-rennes1.fr (E.K.); jean-francois.carpentier@univ-rennes1.fr (J.-F.C.)

Abstract: A synthetic strategy to access asymmetric dinuclear bis(*ansa*-metallocene) pre-catalysts is described. As a key step, the Pd-catalyzed Suzuki cross-coupling of 9,9-*bis*(trimethylsilyl)-fluoren-2-yl-boronic acid with a substituted 2-bromo-9*H*-fluorene generates an asymmetric 2,2′-bifluorene platform, which can be individually functionalized at the two differentiated 9-positions. Herein, as a first demonstration of this strategy, we report the asymmetric dinuclear bis(*ansa*-zirconocene) complex 2,2′-[{Me_2C(Flu)(Cp)}$ZrCl_2$][{Me_2C($^{7\text{-}t\text{Bu}}$Flu)(Cp)}$ZrCl_2$], which has been characterized with NMR spectroscopy and high-resolution mass spectrometry. The performance of this bimetallic pre-catalyst when combined with MAO has been evaluated in ethylene, propylene, and ethylene/1-hexene (co-)polymerization. This pre-catalyst is revealed to be less productive than the mononuclear reference pre-catalyst {Me_2C($^{2,7\text{-}t\text{Bu}}$Flu)(Cp)}$ZrCl_2$, likely because of higher steric hindrance induced by the linkage at the difluorenyl platform. The resulting (co-)polymers featured only slight differences in terms of molecular weights, tacticity, and comonomer incorporation. No bimodal molecular weight distribution was achieved at any produced polymer; this might have originated from the close similarity of the connected Cp/Flu moieties or a rapid chain-transfer phenomenon between the different active sites which were quite close to each other.

Keywords: dinuclear complexes; group 4 metallocenes; olefin polymerization catalysis; copolymers

Citation: Jende, L.N.; Roisnel, T.; Cirriez, V.; Welle, A.; Kirillov, E.; Carpentier, J.-F. An Asymmetric Dinuclear Bis(*ansa*-Zirconocene) Complex: Synthesis and Performance in Olefin (co-)Polymerization. *Catalysts* **2023**, *13*, 1108. https://doi.org/10.3390/catal13071108

Academic Editors: Victorio Cadierno and Raffaella Mancuso

Received: 26 June 2023
Revised: 12 July 2023
Accepted: 13 July 2023
Published: 15 July 2023

1. Introduction

In order to discover unique/more efficient catalytic performances in olefin polymerization processes, a variety of dinuclear group 4 metallocene compounds that contain two covalently linked metallocene units have recently been prepared and reported [1–3]. In some ideal cases, such dinuclear systems may generate, in a one-step process, bimodal distributions made of two inherently different macromolecule populations, differing either in molecular weight, comonomer incorporation, or microstructure (tacticity, branching, etc.). Moreover, in some other cases, 'synergistic/cooperative' effects may arise when the two active metal centers are located at a distance that facilitates effective chemical interactions, eventually resulting in better performance than the mononuclear analogues (higher molecular weights, higher comonomer incorporation, etc.) [2–5]. The most commonly reported bi- or multinuclear group 4 metal pre-catalysts for olefin polymerization are metallocene-type complexes with hydrocarbyl- [4–14] or silyl/silyloxy- [6,15–17] bridges between their cyclopentadienyl-type (Cp) moieties (Chart 1). Such catalysts usually produce atactic poly(α-olefins) (e.g., polypropylene) because of the lack of a stereoselective coordination site. In contrast, it is well known that stereoselectivity via controlled pre-coordination and insertion of the monomer can be achieved with group 4 *ansa*-metallocenes, i.e., complexes that feature one- or two-carbon or silylene-bridged Cp/Ind/Flu (Ind = indenyl; Flu = fluorenyl) moieties. However, dinuclear bis(*ansa*-metallocene)s are rare and are

limited to those linked at the Cp moieties [18] or at the one-C/Si-bridge, [19–21] respectively. To our knowledge, [$CpZrCl_2$(9,9′-$FluCH_2CH{=}CHCH_2Flu$)$CpZrCl_2$], prepared via Grubbs' Ru-catalyzed metathesis reaction from the parent $CpZrCl_2$(9-$FluCH_2CH{=}CH_2$), is one of the two fluorenyl-linked group 4 bis(metallocene) complexes reported so far [9]. In addition, our group prepared trinuclear tris(*ansa*-metallocene) complexes, $Ph[\{Me_2C(2\text{-}Flu^R)(Cp)\}MCl_2]_3$ (M = Zr, Hf) from an original 1,3,5-tris(fluoren-2-yl-R)benzene platform (R = H, 6- or 7-*t*Bu) (Chart 2) [22]. In this work, we probed another synthetic strategy for novel 2,2′-fluorenyl-linked bis(*ansa*-zirconocene)s, enabling access to asymmetric complexes, and report the synthesis, characterization, and performance in olefin (co-)polymerization of a first prototypical example.

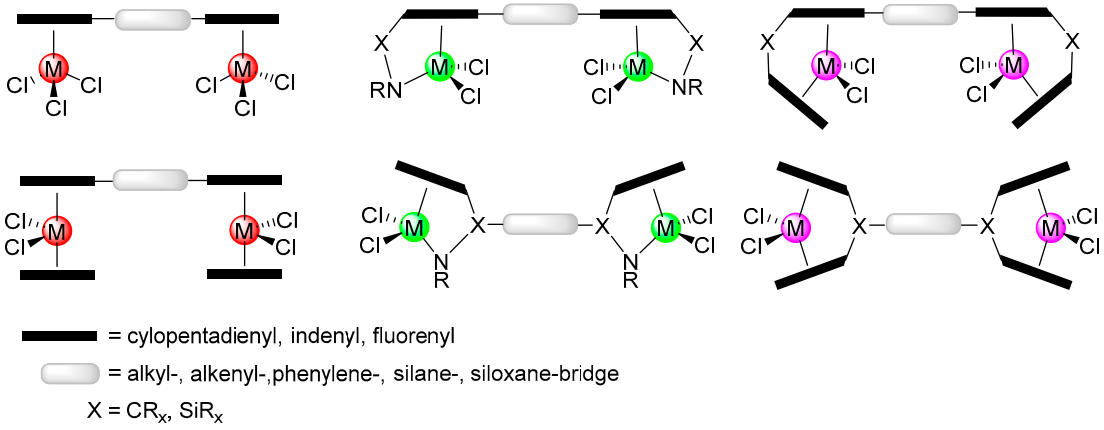

Chart 1. Examples of common dinuclear platforms encountered in group 4 metallocene-type pre-catalysts.

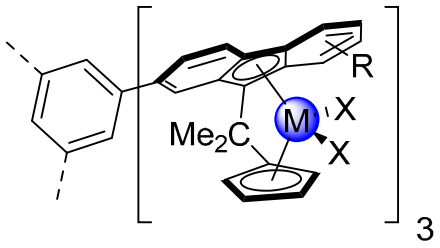

Chart 2. Group 4 tris(*ansa*-metallocene) pre-catalysts reported in previous studies [22].

2. Results and Discussion

2.1. Synthesis of the Asymmetric Bis(Cp/Flu) Proligand and Corresponding Bis(ansa-Zirconocene)

With the aim to generate an asymmetric 2,2′-bifluorene platform, 9,9-*bis*(trimethylsilyl)-(fluoren-2-yl)boronic acid **2** was prepared from 2-bromo-fluorene in a two-step synthesis according to the procedure in the literature (Scheme 1, **i** and **ii**) [23]. As a counterpart to the palladium-catalyzed coupling reaction, 2-bromo-7-*tert*-butyl-fluorene (**4**) was synthesized from 2-acetyl-fluorene (Scheme 1, **iii** and **iv**) [24,25]. Subsequent Suzuki coupling of **2** and **4** delivered the desired 2,2′-bifluorene **5** in good yield (61%, Scheme 1, **v**) [23,26]. Product **5** was fully characterized using 1D and 2D NMR spectroscopy (Figures S7–S9). Single crystals suitable for X-ray diffraction analysis were grown at room temperature from a hot saturated heptane solution, and the molecular structure is shown in Figure 1.

The one-sided trimethylsilyl-protection at bifluorene **5** enabled the selective deprotonation of the other (i.e., the *tert*-butyl-functionalized) fluorenyl moiety, which was then reacted with 6,6-dimethylfulvene to give the mono-(Cp/Flu) compound **6** (Scheme 2, **vi**) [27,28]. Subsequent desilylation of the protected fluorenyl moiety was achieved using potassium hydroxide at elevated temperature (**vii**) [23]. Both mono-(Cp/Flu) bifluorene compounds **6** and **7** were fully characterized using NMR and X-ray diffraction. In particular, the NMR spectra recorded in $CDCl_3$ (Figures S10–S17) show the presence of two tautomers, as indicated by the presence of two signals for the methylene hydrogens of the cyclopentadienyl

fragment (δ^1H = 3.15–3.30 ppm) and for the hydrogen bonded at the sp^3-carbon of the fluorenyl moiety (δ^1H = 4.20–4.32 ppm). Single crystals suitable for X-ray diffraction analysis of **6** and **7** were obtained from hot saturated heptane solutions at room temperature (Figure 2).

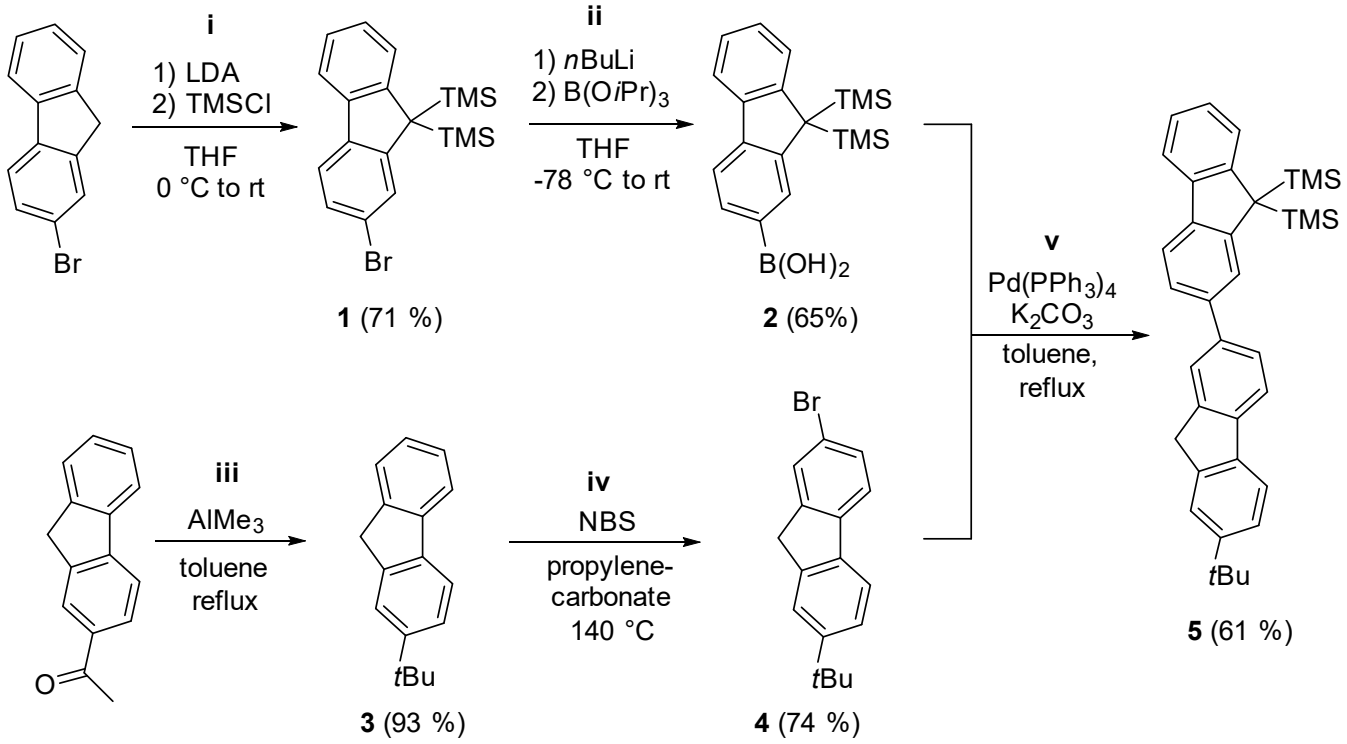

Scheme 1. Synthesis of the asymmetric 2,2′-bifluorene platform **5**.

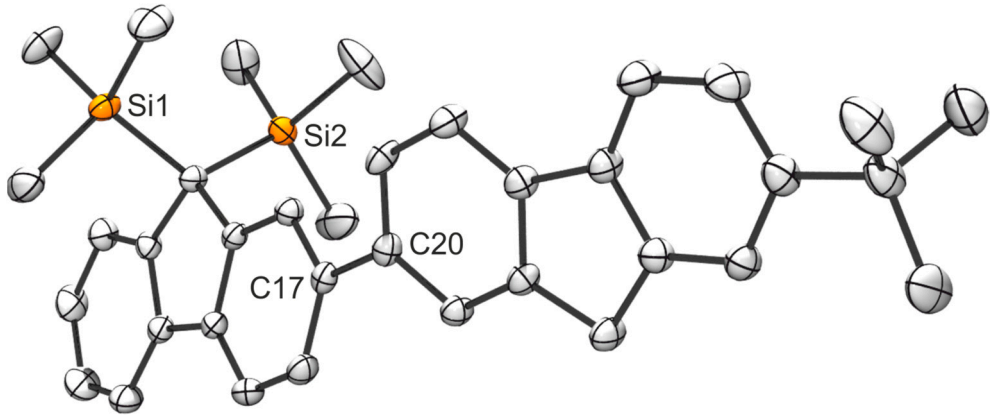

Figure 1. Molecular structure of the asymmetric 2,2′-bifluorene **5**. Atomic displacement parameters are set at the 50% probability level. Hydrogen atoms are omitted for clarity.

Further deprotonation of compound **7** with two equivalents of *n*BuLi and reaction with 6,6-dimethylfulvene gave bis(proligand) **8** in 68% yield (**viii**) [29]. Compound **8** was characterized using NMR spectroscopy, and a complete signal assignment of the recorded ^{1}H and ^{13}C NMR spectra was enabled with additional ^{1}H–^{13}C HSQC and HMBC NMR experiments. The observation of three signals for the 9-*H* Flu hydrogens (δ_H 4.32–4.20) and four signals for the Cp methylene hydrogens at δ_H 3.28 and 3.15 ppm in the ^{1}H NMR spectrum likely accounts for the presence of stereogenic C9 centers (hence two diastereomers) and/or the presence of four possible tautomers of the C = C double bonds in the two different Cp rings.

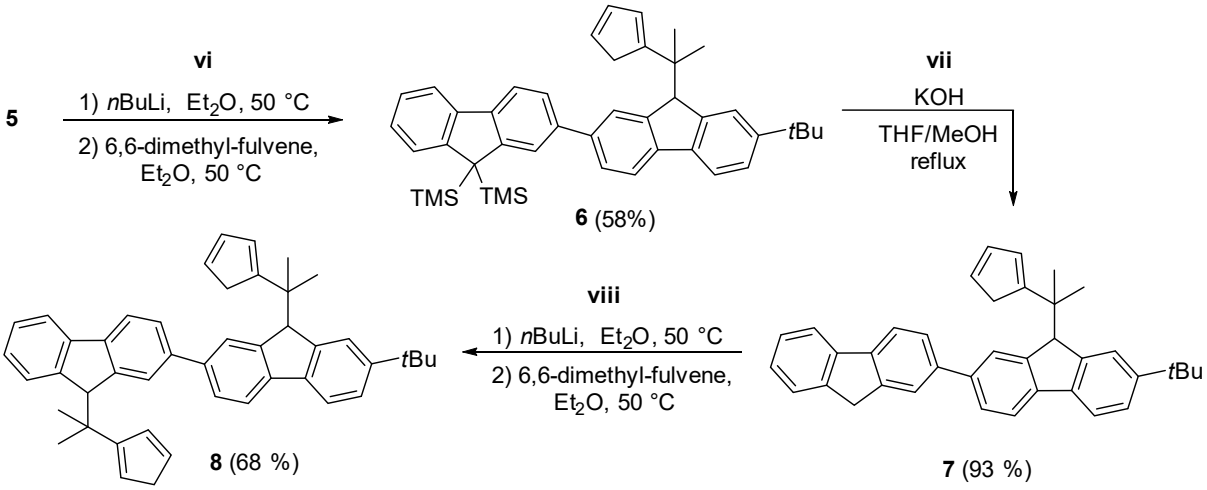

Scheme 2. Synthesis of the bisfluorene-based asymmetric bis(Cp/Flu) proligand **8**.

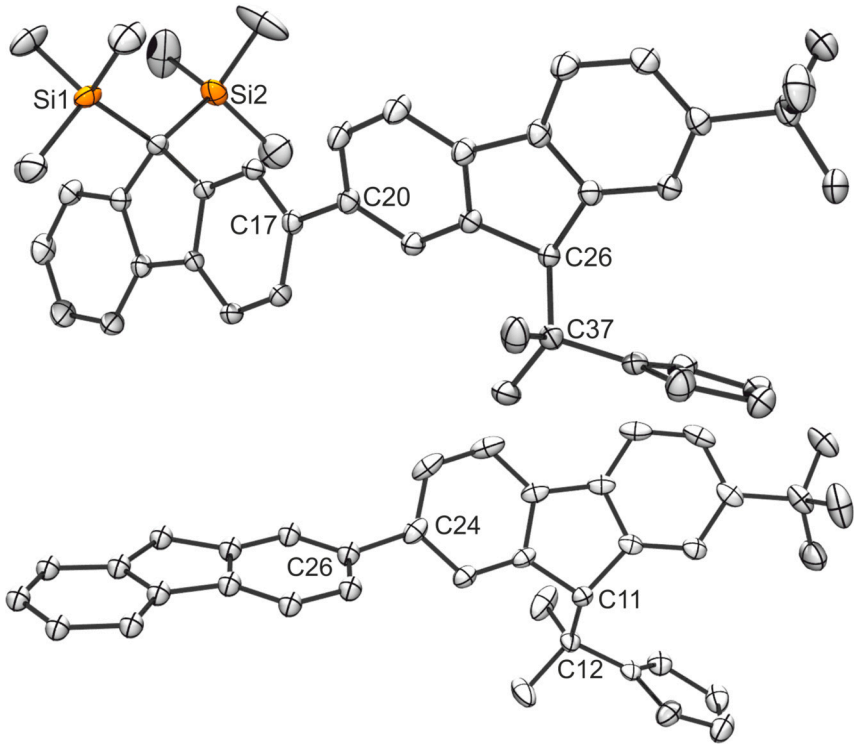

Figure 2. Molecular structures of the protected (**6**, **top**) and desilylated (**7**, **bottom**) $Me_2C(C_5H_5)$ functionalized 2,2′-bifluorenes. Atomic displacement parameters are set at the 50% probability level. Hydrogen atoms are omitted for clarity.

Regular salt metathesis reaction between the ligand tetra-anion, generated in situ from **8** in diethyl ether, and $ZrCl_4$ returned the dinuclear bis(*ansa*-zirconocene dichloride) 2,2′-[{Me_2C(Flu)(Cp)}$ZrCl_2$][{Me_2C($^{7\text{-}t\text{Bu}}$Flu)(Cp)}$ZrCl_2$] (**9**) (Scheme 3). After extraction with dichloromethane and removal of lithium chloride, the zirconium complex was isolated in good yield as a characteristically pink, microcrystalline material. Yet, all attempts to grow single crystals suitable for X-ray diffraction analysis remained unsuccessful. Alternatively, high-resolution mass spectrometry unequivocally evidenced the formation of the bimetallic complex (ASAP–MS and MALDI–ToF-MS, Figures S28 and S29). In addition, the complex was analyzed comprehensively using NMR spectroscopy. Notably, once all solvents had evaporated to complete the dryness of complex **9**, its solubility decreased dramatically; thus, small amounts of diethyl ether and hexane were detected in both the ^{1}H and ^{13}C

NMR data in CD_2Cl_2, yet without hampering full signal assignment (Figures S22–S27). The signals of the cyclopentadienyl moieties are the most informative, with four sharp apparent quartets in the region of δ^1H = 5.72–5.84 ppm (4H), which correlate with four carbon peaks at $\delta^{13}C$ = 101.7–102.8 ppm, and which with the other signals at δ^1H = 6.28–6.36 ppm (4H) account for the eight individual hydrogens in the 2–5-positions at Cp and Cp′. Along with the sum of 44 detected carbon signals, this also means that either only one of the two possible isomers was formed (Scheme 3) or their presence could not be determined with NMR spectroscopy.

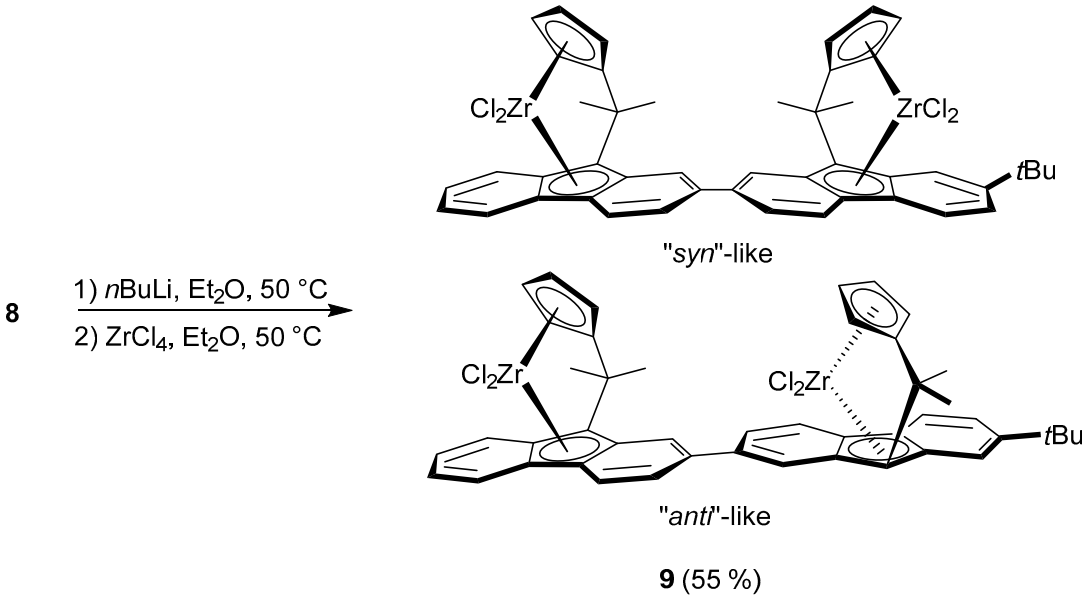

Scheme 3. Synthesis of the asymmetric 2,2′-bisfluorene-linked dinuclear bis(*ansa*-zirconocene) **9** (possible mixture of two diastereomers, "*syn*"- and "*anti*"-like).

DFT computations were conducted to assess the possible geometries of the two C_1-symmetric, "*syn*"- and "*anti*"-like diastereomers of **9** (Figure 3) and their relative energies. These calculations returned only 0.9 kcal·mol^{-1} of energy difference between the two diastereomers, which corresponds to a theoretical "*syn*"/"*anti*" ratio of ca. 5:1 at room temperature. Note, however, that this minimal energy difference falls within the usually accepted range of accuracy of DFT computations (2–3 kcal·mol^{-1}). The two metal centers are located within the same distance (8.726 Å) in both computed diastereomers.

2.2. Olefin (Co-)Polymerization

The dinuclear bis(*ansa*-zirconocene) complex **9**, in combination with MAO, was evaluated in the homogeneous (co-)polymerization of ethylene, propylene, and ethylene/1-hexene (toluene, 4 barg of constant pressure, 20 and 60 °C). Each polymerization experiment was repeated independently two times under the same conditions, revealing good reproducibility in terms of activity (gas uptake) and productivity (polymer yield). For comparison purposes, the catalytic performance of the structurally related mononuclear reference metallocene pre-catalysts $\{Me_2C(^{2,7\text{-}t\text{Bu}}Flu)(Cp)\}ZrCl_2$ (**M**) and $\{Me_2C(Flu)(Cp)\}ZrCl_2$ (**M′**) was determined as well under the same conditions. The productivities of the catalyst are estimated from the polymer yield of the reaction for a short period (15 min) in order to avoid the mass transfer effect.

Selected ethylene polymerization results are summarized in Table 1. For complex **9**, a decrease from 5000 to 2000 equivalents of MAO per metal center had no effect on the catalytic performance, and the recovered polymers exhibited similar physicochemical properties (Table 1, entries 1 and 2). The productivities and the molecular weight distributions were slightly lower or comparable to those of the benchmark mononuclear metallocene complexes **M** and **M′** (entries 4 and 6, respectively). Expectedly, both pre-catalysts **9** and

M showed lower polymerization productivity at 20 °C (entries 3 and 5), whereby only the polymer formed by the reference metallocene could be analyzed, showing a 3-fold increased molecular weight and slightly broader molecular weight distribution compared to the polymer produced at 60 °C (entries 4 and 5).

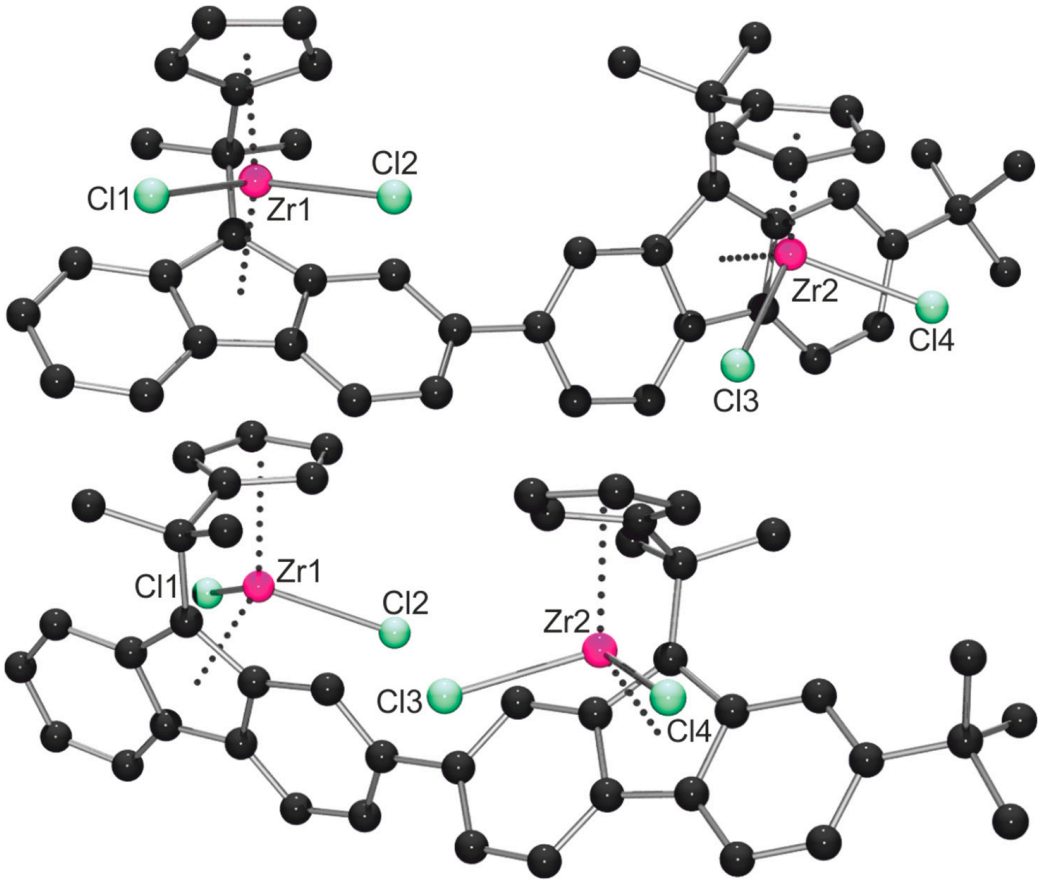

Figure 3. DFT-optimized structures of the two diastereomers of **9** (most stable conformations; top: "*syn*"-like diastereomer; bottom: "*anti*"-like diastereomer). Computed Zr ··· Zr distances: 8.726 Å for the "*syn*"-like diastereomer; 8.727 Å for the "*anti*"-like diastereomer.

Table 1. Ethylene Polymerization [a].

Entry	Precat.	Temp [°C]	[MAO]/[Zr]	m_{polym} [g]	Prod. [kg(PE)·mol(Zr)$^{-1}$·h^{-1}]	T_m [b] [°C]	M_n [c] [kg·mol^{-1}]	M_w/M_n [c]
1	**9**	60	5000	1.74	4640	132.2	43.7	3.3
2	**9**	60	2000	1.71	4560	131.6	48.9	3.1
3	**9**	20	5000	0.14	373	131.1	n.d. [d]	n.d. [d]
4	**M**	60	5000	2.79	7440	132.0	39.4	3.9
5	**M**	20	5000	0.69	1840	133.1	115.5	4.1
6	**M′**	60	5000	2.66	7090	135.1	25.7	3.5

[a] Polymerization conditions: 300 mL high-pressure glass reactor; solvent: toluene, 150 mL; P(ethylene) = 4 barg; [Zr] = 10 µmol·L^{-1}; time = 15 min. [b] Determined with DSC from second run. [c] Determined with SEC in 1,2,4-trichlorobenzene at 135 °C. [d] Not determined.

The performance of pre-catalysts **9**, **M**, and **M′** in propylene polymerization is summarized in Table 2. A decrease in the [MAO]/[Zr] ratio from 5000 to 2000 did not affect the productivity of pre-catalyst **9** but led to a significant increase in the molecular weight of the resulting PP (9.9 vs. 14 kg mol^{-1}, entries 7 and 8), while its dispersity stayed constant. A possible explanation for the observed increase in molecular weight at the low [MAO]/[Zr] ratio is the lower amount of $AlMe_3$ present in the used MAO solution, which is known to act as a chain-transfer reagent. At the polymerization temperature of 60 °C, the dinuclear

9 featured inferior productivity compared to the mononuclear **M** (5690 vs. 25,870 kg(PP) mol(Zr)$^{-1}$ h^{-1}, entries 7 and 10, respectively), though being comparable to that of **M′** (4550 kg(PP) mol(Zr)$^{-1}$ h^{-1}, entry 12). Yet, both metallocenes **9** and **M** featured nearly the same productivity at a polymerization temperature of 20 °C (8300 vs. 7800 kg(PP) mol(Zr)$^{-1}$ h^{-1}, entries 11 and 9). As expected, the dinuclear complex **9** produces highly syndiotactic polypropylene similar to the well-investigated benchmark pre-catalyst **M**; however, its stereoregulation is slightly lower at both polymerization temperatures ([*r*] at 60 °C: 90.4 vs. 92.2%; at 20 °C: 92.9 vs. 96.8%).

Table 2. Propylene Polymerization [a].

Entry	Precat.	Temp [°C]	[MAO]/[Zr]	m_{polym} [g]	Prod. [kg(PP)·mol(Zr)$^{-1}$·h^{-1}]	T_m [b] [°C]	T_{cryst} [b] [°C]	M_n [c] [kg·mol^{-1}]	M_w/M_n [c]	[*rrrr*]/[*rr*]/[*r*] [d] [%]		
7	**9**	60	5000	4.31	5690	102.2 sh118.0 s	56.6	9.9	2.3	70.0	84.1	90.4
8	**9**	60	2000	3.90	5150	102.1 sh118.4 s	48.5	14.3	2.3	69.2	83.4	90.1
9	**9**	20	5000	5.92	7810	119.6 sh135.3 s	75.0	21.7	2.5	78.7	88.4	92.9
10	**M**	60	5000	19.6	25,870	101.7 sh118.9 s	51.1	16.8	2.2	74.7	86.7	92.2
11	**M**	20	5000	6.32	8340	141.5 s150.5 s	97.9	35.5	2.2	89.0	94.8	96.8
12	**M′**	60	5000	3.45	4550	113.1	55.5	13.2	3.6	64.2	79.3	87.7

[a] Polymerization conditions: 300 mL high-pressure glass reactor; solvent: toluene, 150 mL; P(propylene) = 4 barg; [Zr] = 10 μmol·L^{-1}; time = 30 min. [b] Determined with DSC from second run; *sh* and *s* stand for shoulder and strong (endotherms), respectively. [c] Determined with SEC in 1,2,4-trichlorobenzene at 135 °C. [d] Syndiotactic tetrad, triad, and dyad, as determined with ^{13}C NMR spectroscopy.

Table 3 summarizes the performance observed in ethylene/1-hexene copolymerization. The productivity of the catalytic system based on dinuclear metallocene **9** and the molecular weights of the produced copolymers were affected by the [MAO]/[Zr] ratio (entries 13 and 14); this is comparable to the observations made regarding propylene polymerization. Again, this finding might be due to the variable amount of $AlMe_3$ acting as a chain-transfer reagent. The productivity of the dinuclear system decreased drastically when copolymerization was carried out at 20 °C, similar to the observations made during ethylene homopolymerization. The copolymerization productivity of the mononuclear catalytic system based on **M** was less affected by temperature, and this tendency conforms more with the observations made during the propylene polymerization. The copolymer produced with **9**/MAO at 20 °C had about the same C_6 content as that obtained from the **M** system (4.3 and 4.7 mol-%, respectively); yet, the former material had a much broader dispersity than any other copolymer (M_w/M_n = 3.7 vs. 2.6, respectively), and two distinct melting transitions were observed in the DSC trace (see Figure S45). Although the molecular weight distribution of this material remained apparently monomodal, as indicated by the SEC trace (see Figure S35), these observations suggest the presence of two types of macromolecules and, possibly, that the two centers in the catalyst derived from **9** operated in a differentiated manner.

Table 3. Ethylene/1-Hexene Copolymerization [a].

Run	Precat.	Temp [°C]	[MAO]/[Zr]	m_{polym} [g]	Prod. [kg·mol(Zr)$^{-1}$·h^{-1}]	T_m [b] [°C]	M_n [c] [kg·mol^{-1}]	M_w/M_n [c]	C_6 Incorporated [d]		End-Groups [d,e]	
									mol.%	wt.%	sat.	vinyl
13	**9**	60	5000	3.75	10,000	100.5	27.8	2.1	4.7	12.8	5.1	2.0
14	**9**	60	2000	2.50	6650	104.0	31.4	2.1	3.9	10.8	5.8	2.0
15	**9**	20	5000	0.32	853	94.0 113.1	44.2	3.7	4.3	11.9	5.2	0.0
16	**M**	60	5000	8.89	23,700	82.3	29.7	2.4	6.8	17.9	9.0	0.0
17	**M**	20	5000	1.96	5220	95.5	75.8	2.6	4.7	12.9	4.3	0.0

[a] Polymerization conditions: 300 mL high-pressure glass reactor; solvent: toluene, 150 mL; P[ethylene] = 4 barg; 1-hexene = 2.5 mL; [Zr] = 10 μmol·L^{-1}; time = 15 min. [b] Determined with DSC from second run. [c] Determined with GPC in 1,2,4-trichlorobenzene at 135 °C. [d] Determined with ^{13}C NMR spectroscopy. [e] Saturated and vinyl end-groups per 10,000 C atoms.

3. Materials and Methods

3.1. General Considerations

All manipulations (except polymerizations) were performed under a purified argon atmosphere using standard Schlenk techniques or in a glovebox. Solvents were distilled from Na/benzophenone (THF, Et_2O) and Na/K alloy (toluene, pentane) under nitrogen, degassed thoroughly, and stored under nitrogen prior to use. C_6D_6 (>99.5% D, Euroisotop) was vacuum-transferred from Na/K alloy into a storage tube. $CDCl_3$ and CD_2Cl_2 were kept over CaH_2 and vacuum-transferred before use. MAO (30 wt-% solution in toluene, Albermale; contains ca. 10 wt-% of free $AlMe_3$) was used as received. Other starting materials were purchased from Alfa, Strem, Acros, and Aldrich and used as received.

3.2. Instruments and Measurements

NMR spectra of the organic compounds and complex **9** were recorded, respectively, in regular and Teflon-valved NMR tubes on Bruker AM-300 and AM-400 spectrometers (Bruker AXS Handheld Inc., Kennewick, WA, USA) at 25 °C. Chemical shifts are reported in ppm. Assignment of the resonances was made from 2D $^1H-^1H$ COSY, $^1H-^{13}C$ HSQC, and HMBC NMR experiments. Coupling constants are given in Hertz. Elemental analyses (C, H, N) were performed using a Flash EA1112 CHNS Thermo Electron apparatus (Thermo Finnigan Italia S.p.A., Rodano, Italy). DSC measurements were performed on a SETARAM Instrumentation DSC131 differential scanning calorimeter at heating rate of 10 °C·min^{-1}; first and second runs were recorded after cooling to 30 °C; the reported melting temperatures correspond to the second run. SEC analyses of polymer samples were carried out in 1,2,4-trichlorobenzene at 135 °C at the TotalEnergies research center in Feluy (Belgium) using polystyrene standards for universal calibration. ^{13}C NMR analyses of polypropylene and poly(ethylene-*co*-1-hexene) samples were run on a Bruker AM-500 spectrometer (TotalEnergies, Feluy, Belgium) as follows: solutions of ca. 200 mg of polymer in trichlorobenzene/C_6D_6 mixture at 135 °C in 10 mm tubes, inverse-gated experiment, pulse angle = 90 °, delay = 11 s, acquisition time = 1.25 s, number of scans = 6000.

3.3. Computational Studies

The calculations were performed using the Gaussian 09 [30] program employing B3PW91 [31,32] functional and using a standard split-valence basis set def2-SVP [33]. The solvent effects, in our case for diethyl ether, were taken into account during all the calculations using the SMD model [34]. All stationary points were fully characterized via analytical frequency calculations as true minima (all positive eigenvalues). Zero-point vibrational energy corrections (ZPVEs) were estimated with a frequency calculation at the same level of theory, to be considered for the calculation of the total energy values at T = 298 K.

2-Bromo-9,9-bis(trimethylsilyl)-fluorene (1). As described in the literature [23], 2-bromofluorene (4.90 g, 20 mmol, 1.0 equiv) in dry THF (50 mL) was deprotonated using a freshly prepared LDA solution in THF (1.2 eq.) and subsequently reacted with Me_3SiCl (2.72 g, 3.17 mL, 25 mmol, 1.25 equiv) at 0 °C; the deprotonation/silylation sequence was repeated a second time. The reaction mixture was allowed to warm to room temperature overnight, quenched with excess saturated NH_4Cl solution, and extracted with diethyl ether (3 × 50 mL). The organic layers were combined and washed with 0.1 M HCl, saturated sodium bicarbonate, and brine. The diethyl ether solution was dried over sodium sulfate. After removal of solvent, the crude material was recrystallized from refluxing ethanol. After filtration, product **1** was isolated as a colorless powder (5.5 g, 71%). ^1H NMR (400 MHz, $CDCl_3$, 25 °C): δ 7.95–7.86 (m, 1H), 7.80 (d, J = 8.2 Hz, 1H), 7.73 (d, J = 1.7 Hz, 1H), 7.64–7.55 (m, 1H), 7.50 (dd, J = 8.2, 1.8 Hz, 1H), 7.42–7.33 (m, 2H), −0.05 (s, 18H), −0.06 (s, 1H). ^{13}C NMR (100 MHz, $CDCl_3$, 25 °C): δ 149.7, 147.4, 139.2, 139.2, 127.4, 127.3, 126.1, 124.5, 124.4, 121.0, 119.9, 119.5, 44.6, −0.9. Elem. anal. calcd (%) for $C_{19}H_{25}BrSi_2$: C 58.59, H 6.47; found: C 59.05, H 6.88.

(9,9-Bis(trimethylsilyl)-fluoren-2-yl)boronic acid (2). As described in the literature [23], 2-bromo-9*H*-fluorene-9,9-diyl)*bis*(trimethylsilane) (**1**) (1.95 g, 5.0 mmol) in dry THF (30 mL) was deprotonated using *n*BuLi (2.6 mL of a 2.50 M solution in hexane, 6.5 mmol, 1.2 equiv) and subsequently reacted with triisopropylborate (2.3 mL, 10.0 mmol, 2.0 equiv) at −78 °C. After workup and recrystallization from refluxing hexane, compound **2** was obtained as a white powder (1.15 g, 65%). ^{1}H NMR (300 MHz, C_6D_6, 25 °C): δ 7.95 (dd, *J* = 1.7, 0.5 Hz, 1H), 7.72–7.68 (m, 1H), 7.55–7.42 (m, 3H), 7.41 (dd, *J* = 8.2, 1.7 Hz, 2H), 7.24–7.19 (m, 2H), −0.17 (s, 18H). ^{13}C NMR (75 MHz, C_6D_6, 25 °C): δ 148.3, 146.9, 142.5, 140.2, 130.1, 129.6, 126.1, 124.6, 124.3, 120.2, 119.4, 119.1, 44.1, −0.9. Elemental analysis calcd (%) for $C_{19}H_{27}BO_2Si_2$: C 64.39, H 7.68; found: C 64.80, H 7.81.

2-(*tert*-Butyl)-9*H*-fluorene (3). Under argon, $AlMe_3$ (25 mL, 50 mmol) was syringed into a solution of 2-acetyl-fluorene (4.16 g, 20 mmol) in toluene (40 mL). The mixture was refluxed for 14 h and quenched with dilute aqueous HCl. The organic layer was isolated and dried over $MgSO_4$. Removal of the solvent gave product **3** as a pale yellow solid (4.16 g, 93%). ^{1}H NMR (400 MHz, $CDCl_3$, 25 °C): δ 7.77 (ddd, *J* = 16.5, 7.8, 2.5 Hz, 2H), 7.62 (dt, *J* = 2.7, 1.4 Hz, 1H), 7.58–7.53 (m, 1H), 7.46 (dq, *J* = 8.2, 1.9 Hz, 1H), 7.38 (td, *J* = 7.5, 2.4 Hz, 1H), 7.31 (dq, *J* = 7.5, 1.4 Hz, 1H), 3.92 (s, 2H), 1.43 (s, 9H). Elemental analysis calcd (%) for $C_{17}H_{18}$ (222.32): C 91.84, H 8.16; found: C 91.74, H 8.14.

2-Bromo-7-(*tert*-butyl)-9*H*-fluorene (4). A solution of 7-(*tert*-butyl)-9*H*-fluorene (**3**) (3.00 g, 13.2 mmol) and NBS (2.30 g, 13.2 mmol) in propylene carbonate (50 mL) was heated at 140 °C for 2 h. The reaction mixture was then poured into water (100 mL). After filtration and washing with water, the precipitate was dried under vacuum and further purified with silica gel column chromatography using hexanes as eluent. Removal of solvent gave compound **4** as a colorless crystalline powder (2.95 g, 74%). ^{1}H NMR (400 MHz, $CDCl_3$, 25 °C): δ 7.70 (d, *J* = 8.1 Hz, 1H), 7.69 (s, 1H), 7.63 (d, *J* = 8.2 Hz, 1H), 7.61 (s, 1H), 7.51 (d, *J* = 8.1 Hz, 1H), 7.46 (d, *J* = 8.1 Hz, 1H), 3.89 (s, 2H), 1.43 (s, 9H). ^{13}C NMR (100 MHz, $CDCl_3$, 25 °C): δ 150.6, 145.3, 142.9, 140.8, 138.1, 129.8, 128.2, 124.2, 122.0, 120.9, 119.5, 36.9, 34.9, 31.6. Elemental analysis calcd (%) for $C_{17}H_{17}Br$ (300.05): C 67.78, H 5.69; found: C 68.01, H 5.72.

2,2′-(Flu{TMS}$_2$)($^{7\text{-}t\text{Bu}}$FluH$_2$)$_2$ (5). 2-Bromo-7-(*tert*-butyl)-9*H*-fluorene (**4**) (0.82 g, 2.7 mmol), (9,9-*bis*(trimethylsilyl)-9*H*-fluoren-2-yl)boronic acid (**2**) (1.00 g, 2.8 mmol), toluene (30 mL), and aqueous K_2CO_3 solution (10 mL, 2 M) were combined. After degassing of the reaction mixture for 30 min with bubbling argon, $Pd(PPh_3)_4$ (120 mg, 0.10 mmol) was added. The reaction mixture was further degassed for 10 min and then heated to 120 °C for 16 h. After cooling to room temperature, the organic phase was separated, diluted with diethyl ether, and washed with brine. After removal of the solvent, purification with silica column (petroleum ether/CH_2Cl_2 95:5 *v*/*v*) yielded compound **5** as a white solid (873 mg, 61%). ^{1}H NMR (400 MHz, C_6D_6, 25 °C): δ 8.19 (s, 1H), 7.96 (s, 1H), 7.91 (d, *J* = 5.7 Hz, 1H), 7.91–7.88 (m, 1H), 7.85 (s, 1H), 7.75 (d, *J* = 8.3 Hz, 1H), 7.73 (s, 1H), 7.70 (s, 1H), 7.64 (s, 1H), 7.49 (s, 1H), 7.40 (s, 1H), 7.30 (s, 2H), 3.69 (s, 2H), 1.33 (s, 9H), −0.01 (s, 18H). ^{13}C NMR (100 MHz, C_6D_6, 25 °C): δ 149.8, 148.3, 147.9, 144.3, 143.6, 141.1, 140.5, 140.3, 139.6, 139.1, 127.8, 127.6, 126.3, 125.8, 124.6, 124.4, 124.3, 124.1, 124.0, 123.2, 121.9, 120.3, 120.1, 119.6, 44.2, 36.9, 34.6, 31.4, −1.1. Elemental analysis calcd (%) for $C_{36}H_{42}Si_2$: C 81.45, H 7.97; found: C 81.29, H 7.77. ASAP–MS (200 °C) *m*/*z* calcd for $[M + H]^+$: 531.2903, found: 531.2897; calcd for $[M]^+$ 530.2825, found: 530.2826.

2,2′-(Flu{TMS}$_2$){Me$_2$C($^{7\text{-}t\text{Bu}}$FluH)(C$_5$H$_5$)} (6). To a solution of 2,2′-(Flu{TMS}$_2$)($^{7\text{-}t\text{Bu}}$FluH$_2$)$_2$ (**5**) (1.00 g, 1.88 mmol) in dry diethyl ether (25 mL), *n*BuLi (1.0 mL of a 2.3 M solution in hexane, 2.3 mmol) was added dropwise and the mixture stirred at 60 °C for 4 h. Then, 6,6′-dimethylfulvene (260 mg, 2.5 mmol) was added slowly at room temperature, and the resulting red mixture was stirred at room temperature for 16 h. The reaction was quenched with saturated NH_4Cl solution (40 mL) and extracted with diethyl ether, and the combined organic phase was dried over Na_2SO_4/Na_2CO_3. The solvent and the excess of fulvene were removed in vacuum, and the solid residue was washed with petroleum ether to give compound **6** as a white powder (356 mg, 29%). ^{1}H NMR (500 MHz, CD_2Cl_2,

25 °C): δ 8.05 (s, 1H), 8.02 (s, 1H), 7.92 (s, 1H), 7.83 (s, 1H), 7.74 (s, 1H), 7.72 (s, 1H), 7.70 (s, 1H), 7.68 (s, 1H), 7.66 (s, 1H), 7.45 (s, 3H), 7.23 (s, 1H), 7.09 (s, 1H), 6.57 (d, *J* = 37.4 Hz, 1H), 6.12 (d, *J* = 105.7 Hz, 1H), 4.28 (s, 1H), 3.30 (s, 1H), 3.15 (s, 1H), 1.37 (s, 3H), 1.35 (d, *J* = 5.6 Hz, 9H), 0.99 (s, 3H), 0.02 (d, *J* = 7.9 Hz, 18H). ^{13}C NMR (126 MHz, CD_2Cl_2, 25 °C): δ 157.9, 155.6, 149.3, 149.2, 148.2, 148.2, 147.9, 147.9, 146.3, 146.2, 145.5, 145.5, 141.2, 141.1, 140.0, 139.3, 139.3, 139.3, 139.2, 139.2, 139.1, 138.9, 138.9, 134.3, 133.2, 132.2, 131.1, 126.6, 126.1, 126.1, 125.7, 125.2, 125.0, 124.8, 124.6, 124.4, 124.0, 124.0, 123.7, 123.6, 123.5, 123.3, 123.0, 119.9, 119.8, 119.8, 119.4, 119.4, 118.6, 118.6, 58.0, 55.7, 44.3, 41.1, 40.8, 40.6, 39.5, 34.7, 34.6, 31.3, 27.1, 25.9, 23.9, 23.0, −1.1, −1.1. Elemental analysis calcd (%) for $C_{44}H_{52}Si_2$: C 82.96, H 8.23; found: C 82.44, H 7.91. ASAP–MS (200 °C) *m*/*z* calcd for $[M]^+$: 636.3607, found: 636.3606; calcd for $[M - \{Me_2C\}C_5H_5]^+$: 529.2747, found: 529.2739.

2,2′-(FluH$_2$){Me$_2$C($^{7\text{-}t\text{Bu}}$FluH)(C$_5$H$_5$)} (7). A Schlenk flask was charged with a mixture of THF (15 mL), methanol (7 mL), and 2,2′-(Flu{TMS}$_2$){Me$_2$C($^{7\text{-}t\text{Bu}}$FluH)(C$_5$H$_5$)} (**6**) (220 mg, 0.41 mmol) and degassed for 15 min with bubbling argon. Then, KOH flakes (10 mg, 0.18 mmol) were added, and the reaction mixture was heated to reflux for 2 h under argon. The solution was cooled and filtered to isolate compound **7** as white crystals (148 mg, 73%). ^{1}H NMR (500 MHz, $CDCl_3$, 25 °C): δ 7.85 (s, 2H), 7.77 (s, 2H), 7.63 (d, *J* = 44.5 Hz, 4H), 7.57–7.38 (m, 3H), 7.35 (s, 1H), 7.19 (d, *J* = 62.5 Hz, 1H), 7.04 (dq, *J* = 5.1, 1.6 Hz, 1H), 6.74–6.51 (m, 1H), 6.11 (d, *J* = 109.6 Hz, 1H), 4.22 (d, *J* = 23.6 Hz, 1H), 4.00 (s, 2H), 3.21 (d, *J* = 63.5 Hz, 2H), 1.34 (d, *J* = 4.8 Hz, 9H), 1.24 (d, *J* = 4.7 Hz, 3H), 1.08 (d, *J* = 11.9 Hz, 3H). ^{13}C NMR (126 MHz, $CDCl_3$, 25 °C): δ 158.1, 155.7, 149.3, 149.1, 146.1, 145.5, 143.9, 143.5, 143.4, 141.5, 141.3, 141.2, 140.6, 140.5, 140.3, 139.0, 138.7, 138.6, 134.3, 133.4, 132.3, 131.1, 126.8, 126.7, 126.6, 126.1, 126.0, 125.9, 125.8, 125.1, 125.0, 124.9, 124.8, 124.0, 124.0, 123.7, 123.6, 123.4, 123.2, 120.1, 119.9, 119.4, 119.3, 118.8, 118.7, 58.1, 55.7, 41.1, 40.8, 40.7, 39.6, 37.0, 34.8, 34.8, 31.5, 31.5, 23.9. Elemental analysis calcd (%) for $C_{38}H_{36}$: C 92.64, H 7.36; found: C 92.74, H 7.14. ASAP–MS (230 °C) *m*/*z* calcd for $[M]^+$: 492.2817, found: 429.2813; calcd for $[M - \{Me_2C\}C_5H_5]^+$: 385.1956, found: 385.1956.

2,2′-{Me$_2$C(FluH)(C$_5$H$_5$)}{Me$_2$C($^{7\text{-}t\text{Bu}}$FluH)(C$_5$H$_5$)} (8). To a solution of 2,2′-{FluH$_2$}{Me$_2$C($^{7\text{-}t\text{Bu}}$FluH)(C$_5$H$_5$)} (**7**) (150 mg, 0.30 mmol) in dry diethyl ether (10 mL), *n*BuLi (0.27 mL of a 2.5 M solution in hexane, 0.67 mmol, 2.1 eq.) was added dropwise and the mixture stirred at 60 °C for 3 h. A solution of 6,6′-dimethylfulvene (35.5 mg, 0.33 mmol) in diethyl ether (1 mL) was added slowly at room temperature, and the resulting red mixture was stirred at 60 °C for 2 h. The reaction was quenched with saturated NH_4Cl solution (40 mL) and extracted with diethyl ether, and the combined organic phase was dried over Na_2SO_4/Na_2CO_3. After removal of the solvent and excess of fulvene in vacuum, the solid residue was washed with petroleum ether to give proligand **8** as a white powder (140 mg, 78%). ^{1}H NMR (400 MHz, CD_2Cl_2, 25 °C): δ 7.79 (s, 3H), 7.69 (s, 1H), 7.60 (s, 3H), 7.41 (s, 3H), 7.24 (s, 3H), 7.05 (s, 1H), 6.72 (s, 1H), 6.61 (s, 1H), 6.53 (s, 1H), 6.22 (s, 1H), 6.00 (s, 1H), 4.32–4.20 (m, 2H), 3.28 (d, *J* = 6.9 Hz, 2H), 3.15 (d, *J* = 9.5 Hz, 2H), 1.34 (d, *J* = 4.4 Hz, 9H), 1.25 (d, *J* = 23.2 Hz, 6H), 1.10 (d, *J* = 20.9 Hz, 3H), 1.02 (s, 3H). ^{13}C NMR (101 MHz, CD_2Cl_2, 25 °C): δ 158.0, 157.8, 155.6, 155.4, 149.3, 149.2, 146.1, 146.0, 145.7, 145.5, 141.7, 141.1, 140.9, 138.9, 134.3, 133.3, 132.2, 131.1, 127.1, 126.6, 126.1, 125.9, 125.0, 124.8, 124.0, 123.3, 119.5, 119.3, 119.3, 118.6, 58.0, 55.7, 41.0, 40.8, 40.5, 39.5, 34.6, 31.2, 26.7, 26.1, 25.5, 24.9, 24.3, 23.3. Elemental analysis calcd (%) for $C_{46}H_{46}$: C 92.26, H 7.74; found: C 92.66, H 7.31. ASAP–MS (230 °C) *m*/*z* calcd for $[M]^+$: 598.3599, found: 598.3599; calcd for $[M + H]^+$: 599.3677, found: 599.3677; calcd for $[M - \{Me_2C\}C_5H_5]^+$): 491.2739, found: 491.2732.

[2,2′-{Me$_2$C(Flu)(C$_5$H$_4$)}ZrCl$_2$][{Me$_2$C($^{7\text{-}t\text{Bu}}$Flu)(C$_5$H$_4$)}ZrCl$_2$] (9). In a Schlenk flask, 2,2′-{Me$_2$C(FluH)(C$_5$H$_5$)}{Me$_2$C($^{7\text{-}t\text{Bu}}$FluH)(C$_5$H$_5$)} (**8**) (80 mg, 133 μmol) was suspended in dry diethyl ether (10 mL), *n*BuLi (0.23 mL of a 2.5 M solution in hexane, 0.588 mmol, 4.4 equiv) was added dropwise, and the mixture was stirred at room temperature overnight. Then, zirconium tetrachloride (62 mg, 266 μmol, 2.0 equiv) was added, and the resulting purple/red mixture was stirred at 50 °C for 24 h. Diethyl ether was removed in vacuum, and the solid residue was suspended in CH_2Cl_2 (30 mL). The suspension was filtered over celite© under argon. Removal of the solvent in vacuum gave the desired dimeric

ansa-metallocene complex **9** as a pink powder (82 mg, 67%). ^{1}H NMR (400 MHz, CD_2Cl_2, 25 °C): δ 8.30–8.21 (m, 2H), 8.21–8.17 (m, 1H), 8.12 (s, 1H), 7.96 (s, 1H), 7.84 (s, 3H), 7.73 (s, 4H), 7.63 (s, 1H), 7.35 (s, 1H), 6.38–6.26 (m, 4H), 5.84 (d, *J* = 2.3 Hz, 1H), 5.81 (d, *J* = 2.4 Hz, 1H), 5.79 (d, *J* = 2.4 Hz, 1H), 5.72 (d, *J* = 2.4 Hz, 1H), 2.46 (d, *J* = 4.2 Hz, 6H), 2.41 (s, 6H), 1.41 (s, 9H). ^{13}C NMR (101 MHz, CD_2Cl_2, 25 °C) (some may superimpose): δ 152.8, 143.7, 143.1, 129.5, 125.7, 125.5, 125.4, 125.3, 125.2, 125.1, 124.4, 124.2, 124.1, 123.7, 123.5, 123.5, 123.4, 122.3, 122.2, 121.9, 121.9, 121.8, 119.6, 119.6, 119.4, 119.2, 115.0, 114.6, 103.3, 102.7, 102.7, 102.2, 79.9, 79.4, 41.0, 40.9, 35.8, 31.1, 29.3, 29.1, 29.1, 28.9 (66.1, 15.5: residual Et_2O; 32.2, 23.3, 14.4: residual *n*-hexane). Elem. anal. calcd (%) for $C_{46}H_{42}Cl_4Zr_2$: C 60.11, H 4.61; found: C 58.99, H 4.42. ASAP–MS (300 °C) *m*/*z* calcd for $[MH]^+$: 919.0187, found: 919.0189. MALDI–ToF-MS (DCTB) *m*/*z* calcd for $[M - Cl]^+$: 883.041, found: 883.041.

4. Conclusions

We have developed an effective synthetic strategy to access asymmetric difluorenyl-linked dinuclear bis(*ansa*-metallocene)s. As a first prototypical example, a di-*ansa*-{Cp/Flu-Cp/Flu′} dizirconocene complex has been synthesized. Preliminary investigations on the performance of this bimetallic pre-catalyst in ethylene, propylene, and ethylene/1-hexene (co-)polymerization revealed, in most cases, lower productivity in comparison with a mononuclear reference pre-catalyst $\{Me_2C(^{2,7\text{-}t\text{Bu}}Flu)(Cp)\}ZrCl_2$; this might have resulted from a higher steric hindrance in the dinuclear bis(*ansa*-metallocene) due to the direct linkage in the difluorenyl platform [9]. On the other hand, only slight differences were noticed between the two pre-catalyst systems in terms of molecular weights, tacticity, and comonomer incorporation in the resulting (co-)polymers. No bimodal molecular weight distribution was achieved at any produced polymer. This might have originated from the too-close similarity of the connected Cp/Flu moieties or a rapid chain-transfer phenomenon between the two different active sites which were at a quite close distance from each other. To gain further insights, the synthesis of proligands and the corresponding dinuclear bis(*ansa*-metallocene)s with more differentiated catalytically active metal centers are the subject of current investigations.

Supplementary Materials: The following supporting information can be downloaded at: https://www.mdpi.com/article/10.3390/catal13071108/s1. ^{1}H, ^{13}C, and 2D NMR spectra of organic compounds and complex **9**, mass spectra of complex **9**, crystallographic data for compounds **5**, **6**, and **7** (CCDC 2268879, 2268880, 2268881, respectively), representative SEC, DSC traces, and ^{13}C NMR spectra of homo- and copolymers.

Author Contributions: L.N.J. designed and performed the experimental work and wrote the preliminary draft. T.R. conducted the crystallographic studies. V.C. and A.W. co-supervised the work and contributed to the evolution of the initial project. E.K. conducted the DFT studies. J.-F.C. edited the initial draft. E.K. and J.-F.C. directed the research and finalized the manuscript. All authors contributed to various sections of the manuscript. All authors have read and agreed to the published version of the manuscript.

Funding: This research was funded by TotalEnergies (postdoctoral fellowship to LNJ).

Data Availability Statement: All available data have been made available through the Supplementary Material.

Acknowledgments: We thank Philippe Jehan for the MS analyses. Part of this work has been performed using mass and NMR spectrometers belonging to the CRMPO (UAR ScanMAT, CNRS-Université de Rennes) core facility.

Conflicts of Interest: The authors declare no conflict of interest in the present work.

References

1. Ainooson, M.; Meyer, F. Bimetallic Approaches in Olefin Polymerization and Metathesis. In *Comprehensive Inorganic Chemistry II*, 2nd ed.; Elsevier: Amsterdam, The Netherlands, 2013; pp. 433–458.
2. Delferro, M.; Marks, T.J. Multinuclear olefin polymerization catalysts. *Chem. Rev.* **2011**, *111*, 2450–2485. [CrossRef] [PubMed]

3. McInnis, J.P.; Delferro, M.; Marks, T.J. Multinuclear Group 4 catalysis: Olefin polymerization pathways modified by strong metal–metal cooperative effects. *Acc. Chem. Res.* **2014**, *47*, 2545–2557. [CrossRef] [PubMed]
4. Jüngling, S.; Müllhaupt, R.; Plenio, H. Cooperative effects in binuclear zirconocenes: Their synthesis and use as catalyst in propene polymerization. *J. Organomet. Chem.* **1993**, *460*, 191–195. [CrossRef]
5. Yan, X.; Chernega, A.; Green, M.L.H.; Sanders, J.; Souter, J.; Ushioda, T. Proximity and cooperativity effects in binuclear d^0 olefin polymerization catalysis. Theoretical analysis of structure and reaction mechanism. *J. Mol. Catal. A Chem.* **1998**, *128*, 119–141. [CrossRef]
6. Noh, S.K.; Kim, J.; Jung, J.; Ra, C.S.; Lee, D.-h.; Lee, H.B.; Lee, S.W.; Huh, W.S. Syntheses of polymethylene bridged dinuclear zirconocenes and investigation of their polymerisation activities. *J. Organomet. Chem.* **1999**, *580*, 90–97. [CrossRef]
7. Lee, H.-W.; Park, Y.-H. Polymerization characteristics of in situ supported pentamethylene bridged dinuclear zirconocenes. *Catal. Today* **2002**, *74*, 309–320. [CrossRef]
8. Noh, S.K.; Kim, S.; Yang, Y.; Lyoo, W.S.; Lee, D.-h. Preparation of syndiotactic polystyrene using the doubly bridged dinuclear titanocenes. *Eur. Polym. J.* **2004**, *40*, 227–235. [CrossRef]
9. Kuwabara, J.; Takeuchi, D.; Osakada, K. Zr/Zr and Zr/Fe dinuclear complexes with flexible bridging ligands. Preparation by olefin metathesis reaction of the mononuclear precursors and properties as polymerization catalysts. *Organometallics* **2005**, *24*, 2705–2712. [CrossRef]
10. Lee, M.H.; Kim, S.K.; Do, Y. Biphenylene-bridged dinuclear group 4 metal complexes: Enhanced polymerization properties in olefin polymerization. *Organometallics* **2005**, *24*, 3618–3620. [CrossRef]
11. Liu, X.; Sun, J.; Zhang, H.; Xiao, X.; Lin, F. Ethylene polymerization by novel phenylenedimethylene-bridged homobinuclear titanocene/MAO systems. *Eur. Polym. J.* **2005**, *41*, 1519–1524. [CrossRef]
12. Noh, S.K.; Jung, W.; Oh, H.; Lee, Y.R.; Lyoo, W.S. Synthesis and styrene polymerization properties of dinuclear half-titanocene complexes with xylene linkage. *J. Organomet. Chem.* **2006**, *691*, 5000–5006. [CrossRef]
13. Xiao, X.; Sun, J.; Li, X.; Li, H.; Wang, Y. Binuclear titanocenes linked by the bridge combination of rigid and flexible segment: Synthesis and their use as catalysts for ethylene polymerization. *J. Mol. Catal. A Chem.* **2007**, *267*, 86–91. [CrossRef]
14. Linh, N.T.B.; Huyen, N.T.D.; Noh, S.K.; Lyoo, W.S.; Lee, D.-H.; Kim, Y. Preparation of new dinuclear half-titanocene complexes with *ortho*- and *meta*-xylene linkages and investigation of styrene polymerization. *J. Organomet. Chem.* **2009**, *694*, 3438–3443. [CrossRef]
15. Reddy, K.P.; Petersen, J.L. Synthesis and characterization of binuclear zirconocene complexes linked by a bridge bis(cyclopentadienyl) ligand. *Organometallics* **1989**, *8*, 2107–2113. [CrossRef]
16. Noh, S.K.; Byun, G.-g.; Lee, C.-s.; Lee, D.; Yoon, K.-b.; Kang, K.S. Synthesis, characterization, and reactivities of the polysiloxane-bridged binuclear metallocenes tetramethyldisiloxanediylbis(cyclopentadienyltitanium trichloride) and hexamethyltrisiloxanediylbis(cyclopentadienyltitanium trichloride). *J. Organomet. Chem.* **1996**, *518*, 1–6. [CrossRef]
17. Xu, S.; Huang, J. Asymmetric binuclear metallocene complexes and their application for olefin polymerization. *J. Appl. Polym. Sci.* **2013**, *130*, 2891–2900. [CrossRef]
18. Murray, R.E.; Jayaratne, K.C.; Yang, Q.; Martin, J.L. To Chevron Phillips Chemical Company. WO Pat. 2009/085129, 2009.
19. Soga, K.; Ban, H.T.; Uozumi, T. Synthesis of a dinuclear *ansa*-zirconocene catalyst having a biphenyl bridge and application to ethene polymerization. *J. Mol. Catal. A Chem.* **1998**, *128*, 273–278. [CrossRef]
20. Spaleck, W.; Küber, F.; Bachmann, B.; Fritze, C.; Winter, A. New bridged zirconocenes for olefin polymerization: Binuclear and hybrid structures. *J. Mol. Catal. A Chem.* **1998**, *128*, 279–287. [CrossRef]
21. Alt, H.G.; Ernst, R.; Böhmer, I.K. Dinuclear *ansa*-zirconocene complexes containing a sandwich and a half-sandwich moiety as catalysts for the polymerization of ethylene. *J. Organomet. Chem.* **2002**, *658*, 259–265. [CrossRef]
22. Jende, L.N.; Vantomme, A.; Welle, A.; Brusson, J.-M.; Carpentier, J.-F.; Kirillov, E. Trinuclear tris(*ansa*-metallocene) complexes of zirconium and hafnium for olefin polymerization. *J. Organomet. Chem.* **2018**, *878*, 19–29. [CrossRef]
23. Dane, E.L.; Swager, T.M. Carbanionic route to electroactive carbon-centered anion and radical oligomers. *Org. Lett.* **2010**, *12*, 4324–4327. [CrossRef] [PubMed]
24. Chai, J.; Abboud, K.A.; Miller, S.A. Sterically expanded CGC catalysts: Substituent effects on ethylene and α-olefin polymerization. *Dalton Trans.* **2013**, *42*, 9139–9147. [CrossRef]
25. Tang, W.; Singh, S.P.; Ong, K.H.; Chen, Z.-K. Synthesis of thieno[3,2-*b*]thiophene derived conjugated oligomers for field-effect transistors applications. *J. Mat. Chem.* **2010**, *20*, 1497–1505. [CrossRef]
26. Wolfe, J.P.; Singer, R.A.; Yang, B.H.; Buchwald, S.L. Highly active palladium catalysts for Suzuki coupling reactions. *J. Am. Chem. Soc.* **1999**, *121*, 9550–9561. [CrossRef]
27. Ewen, J.A.; Jones, R.L.; Razavi, A.; Ferrara, J.D. Syndiospecific propylene polymerizations with Group IVB metallocenes. *J. Am. Chem. Soc.* **1988**, *110*, 6255–6256. [CrossRef]
28. Razavi, A.; Ferrara, J. Preparation and crystal structures of the complexes (η^5-$C_5H_4CMe_2\eta^5$-$C_{13}H_8$)MCl_2 (M = Zr, Hf) and their role in the catalytic formation of syndiotactic polypropylene. *J. Organomet. Chem.* **1992**, *435*, 299–310. [CrossRef]
29. Kirillov, E.; Marquet, N.; Razavi, A.; Belia, V.; Hampel, F.; Roisnel, T.; Gladysz, J.A.; Carpentier, J.-F. New C_1-symmetric Ph_2C-bridged multisubstituted *ansa*-zirconocenes for highly isospecific propylene polymerization: Synthetic approach via activated fulvenes. *Organometallics* **2010**, *29*, 5073–5082. [CrossRef]

30. Frisch, M.J.; Trucks, G.W.; Schlegel, H.B.; Scuseria, G.E.; Robb, M.A.; Cheeseman, J.R.; Scalmani, G.; Barone, V.; Mennucci, B.; Petersson, G.A.; et al. *Gaussian 09, Revision, D.01*; Gaussian Inc.: Pittsburgh, PA, USA, 2009.
31. Becke, A.D. Density-functional exchange-energy approximation with correct asymptotic behavior. *Phys. Rev. A* **1988**, *38*, 3098–3100. [CrossRef] [PubMed]
32. Becke, A.D. Density-functional thermochemistry. III. The role of exact exchange. *J. Chem. Phys.* **1993**, *98*, 5648–5652. [CrossRef]
33. Weigend, F.; Ahlrichs, R. Balanced basis sets of split valence, triple zeta valence and quadruple zeta valence quality for H to Rn: Design and assessment of accuracy. *Phys. Chem. Chem. Phys.* **2005**, *7*, 3297–3305. [CrossRef]
34. Marenich, A.V.; Cramer, C.J.; Truhlar, D.G. Universal solvation model based on solute electron density and on a continuum model of the solvent defined by the bulk dielectric constant and atomic surface tensions. *J. Phys. Chem. B* **2009**, *113*, 6378–6396. [CrossRef] [PubMed]